PHILOSOPHICAL TRANSACTIONS OF THE ROYAL SOCIETY A

rsta.royalsocietypublishing.org

Research

Cite this article: Parish MM. 2014 Magnetocapacitance without magnetism. *Phil. Trans. R. Soc. A* **372**: 20120452. http://dx.doi.org/10.1098/rsta.2012.0452

One contribution of 10 to a Theme Issue 'Magnetoelectric phenomena and devices'.

Subject Areas:
solid state physics, electromagnetism

Keywords:
magnetodielectric effect, composite media, magnetotransport, Maxwell–Wagner effect

Author for correspondence:
Meera M. Parish
e-mail: meera.parish@ucl.ac.uk

Magnetocapacitance without magnetism

Meera M. Parish

London Centre for Nanotechnology, Gordon Street, London WC1H 0AH, UK

A substantial magnetodielectric effect is often an indication of coupled magnetic and elastic order, such as is found in the multi-ferroics. However, it has recently been shown that magnetism is not necessary to produce either a magnetoresistance or a magnetocapacitance when the material is inhomogeneous. Here, we will investigate the characteristic magnetic-field-dependent dielectric response of such an inhomogeneous system using exact calculations and numerical simulations of conductor–dielectric composites. In particular, we will show that even simple conductor–dielectric layers exhibit a magneto-capacitance, and thus random bulk inhomogeneities are not a requirement for this effect. Indeed, this work essentially provides a natural generalization of the Maxwell–Wagner effect to finite magnetic field. We will also discuss how this phenomenon has already been observed experimentally in some materials.

1. Introduction

Macroscopic inhomogeneities can have a surprising impact on the magnetotransport of a material. A spectacular example of this is the anomalous transverse magnetoresistance observed in doped silver chalcogenides [1,2]. Here, the presence of inhomogeneities distorts the current paths in such a way that the Hall part is mixed into the longitudinal part of the response, thus giving rise to a large, linear magnetoresistance that persists across a range of magnetic fields and temperatures [3,4]. Because this is a classical effect that does not require magnetism, it is relatively insensitive to temperature and thus potentially useful for technological applications. Indeed, inhomogeneities have already been exploited in the design of magnetic sensors: semiconductor devices with 'extraordinary

Royal Society Publishing

magnetoresistance' rely on the presence of a metallic inclusion to distort current and increase the device's resistance in a magnetic field [5,6].

There are similar non-trivial effects in the case of the AC dielectric response: Catalan [7] has shown that a material can display a substantial magnetocapacitance when an intrinsic magnetoresistance is combined with Maxwell–Wagner extrinsic effects such as contact effects and bulk inhomogeneities. Subsequently, Parish & Littlewood [8] showed that a magnetocapacitance can be induced by inhomogeneities alone and magnetism is not even necessary. In particular, we found that a finite magnetic field induced a characteristic dielectric *resonance*, though no inductive element was present in the system. As we discuss below, this is a counterintuitive phenomenon that every experimentalist should be aware of when probing the dielectric response of a material, particularly given that the existence of a magnetocapacitance is often taken as an indication of coupled ferroelectric and magnetic order. It is already known that composites consisting of a ferroelectric and a ferromagnet can generate a magnetoelectric coupling in the absence of any intrinsic coupling [9]. Here, we examine how simple conductor–dielectric composites can yield a dielectric response that depends on magnetic field in the absence of any magnetic or ferroelectric order. This effect is insensitive to the microscopics and is thus generic, being dependent only on the distribution of local capacitive and conductive regions. The only relevant material parameters are the static dielectric constant ε of the capacitive regions and the resistivity tensor $\hat{\rho}$ (or conductivity tensor $\hat{\sigma} \equiv \hat{\rho}^{-1}$) in the conducting regions. As such, this magnetodielectric effect can occur in a variety of inhomogeneous materials: for instance, it has already been observed experimentally in nanoporous silicon [10,11] and potentially in the manganite $La_{2/3}Ca_{1/3}MnO_3$ [12], as discussed in §5.

In the following, we will investigate the characteristic magnetic-field-dependent dielectric response of two-dimensional conductor–dielectric composites using exact calculations, numerical simulations and the effective medium approximation. In particular, we will show that even simple conductor–dielectric layers exhibit a magnetocapacitance, and thus random inhomogeneities in the bulk are not a requirement for this effect. Rather, it is sufficient to have conductor–dielectric interfaces that are perpendicular to the overall flow of current (or the movement of charges). This also appears to be consistent with experiment, because there is an observed link between magnetocapacitance and interfaces with free charges [13]. We will also discuss how an intrinsic magnetoresistance could enhance this effect.

2. Model and methods

We consider a classical two-dimensional composite medium consisting of purely dielectric regions (defined by dielectric constant ε) and purely conducting regions. The latter regions have the following resistivity tensor in a transverse magnetic field $\mathbf{H} = H\hat{z}$:

$$\hat{\rho} = \begin{pmatrix} \rho_{xx} & \rho_{xy} \\ -\rho_{xy} & \rho_{xx} \end{pmatrix}, \tag{2.1}$$

where we have assumed that the conductor is isotropic. We focus on the simplest case where $\rho_{xx} = \rho$ and $\rho_{xy}/\rho = \mu H \equiv \beta$, with μ the carrier mobility. Locally, the current $\mathbf{j}(\omega, \mathbf{r})$ is related to the electric field $\mathbf{E}(\omega, \mathbf{r})$ via Ohm's law $\mathbf{E}(\omega, \mathbf{r}) = \hat{\rho}(\omega, \mathbf{r})\mathbf{j}(\omega, \mathbf{r}) \equiv (\mathrm{i}\omega\hat{\varepsilon}(\omega, \mathbf{r}))^{-1}\mathbf{j}(\omega, \mathbf{r})$, and globally the system is driven by electric field $\langle \mathbf{E}(\omega) \rangle$ at frequency ω, where $\langle \cdots \rangle$ corresponds to a volume average. The measured response averaged over the whole system is then the effective resistivity defined from $\langle \mathbf{E}(\omega) \rangle = \hat{\rho}_e(\omega)\langle \mathbf{j}(\omega) \rangle$. For the standard experimental set-up where the boundary conditions are such that $\langle j_y \rangle = 0$ as in figure 1*a*, the components of the dielectric function that are actually probed are then given by $\varepsilon_{xx}(\omega) = (\mathrm{i}\omega\rho_{e,xx}(\omega))^{-1}$ and $\varepsilon_{xy}(\omega) = (\mathrm{i}\omega\rho_{e,xy}(\omega))^{-1}$. The longitudinal response $\varepsilon_{xx}(\omega)$ is the usual dielectric response measured in experiment, whereas the transverse response $\varepsilon_{xy}(\omega)$ can be extracted from a measurement of the transverse electric field $E_y(\omega) = E_x(\omega)\varepsilon_{xx}(\omega)/\varepsilon_{xy}(\omega)$.

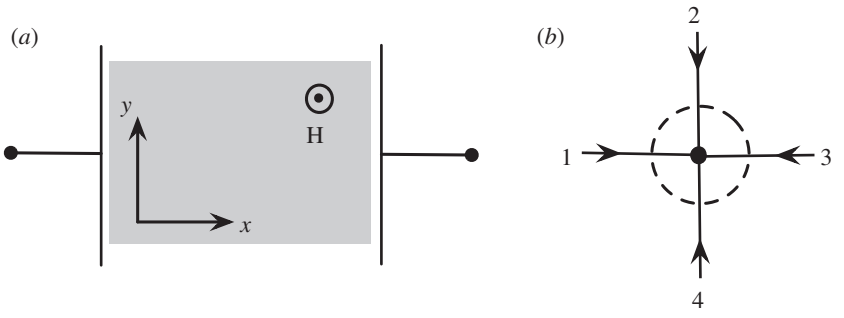

Figure 1. The basics of probing and modelling dielectric response. (*a*) Diagram depicts the general measuring set-up, where a rectangular sample is subjected to an oscillating electric field $E_x\hat{x}$ and a static transverse magnetic field H. The response of a general two-dimensional conductor–dielectric composite can be simulated with a network of four-terminal elements (*b*).

For the isotropic two-component media considered in §4, one can make use of the self-consistent effective medium approximation outlined in references [14–16]. Here, we first imagine that we have a single inclusion embedded in an effective medium, and then we average over all inclusions to self-consistently determine the response of this effective medium. This amounts to solving the coupled equations

$$\sum_i p_i(\hat{\sigma}_i - \hat{\sigma}_e)\left(1 + \frac{\hat{\sigma}_i - \hat{\sigma}_e}{2\sigma_{e,xx}}\right) = 0, \tag{2.2}$$

where $\hat{\sigma}_e = \hat{\rho}_e^{-1}$ and p_i is the volume fraction of the ith component. For the special case where the fractions are equal ($p_1 = p_2 = 1/2$), we can exploit a symmetry transformation for the electric field and current density [17–19] to derive an *exact* result for the effective dielectric function of the composite medium [8]. Note that the effective medium approximation recovers this exact result for equal fractions, and becomes formally exact in the limits $p_1 \to 0$, $p_2 \to 0$. Thus, we expect it to provide an accurate approach for investigating isotropic media across all volume fractions.

For composites with anisotropic inhomogeneities such as the conductor–dielectric layers in §3, one requires a more brute force numerical approach. In this case, we discretize the system into four-terminal elements as shown in figure 1*b*, where the voltages V_i at the terminals of each element are linearly related to the currents I_i via an impedance matrix: $V_i = Z_{ij}I_j$. Note that each voltage is defined with respect to the element centre and incoming currents are defined as positive. In a purely conducting region, $Z_{ij} = (\rho/2)(\delta_{ij} + \beta M_{ij})$, where

$$M_{ij} = \frac{1}{2}\begin{pmatrix} 0 & -1 & 0 & 1 \\ 1 & 0 & -1 & 0 \\ 0 & 1 & 0 & -1 \\ -1 & 0 & 1 & 0 \end{pmatrix}. \tag{2.3}$$

In a purely dielectric region, we simply have $Z_{ij} = (2\mathrm{i}\omega\varepsilon)^{-1}\delta_{ij}$. To simulate a given layered composite such as in figure 2, we construct an $N \times M$ rectangular network of these four-terminal elements and then take the limit of large N and M (keeping N/M and the proportions of each phase fixed). In general, the response converges rapidly to that of an infinite network.

3. Conductor–dielectric interfaces

In this section, we consider simple conductor–dielectric layers (figure 2), which constitute the simplest realization of anisotropic inhomogeneities. They also allow us to investigate the behaviour of conductor–dielectric interfaces and they can thus potentially describe the effect of

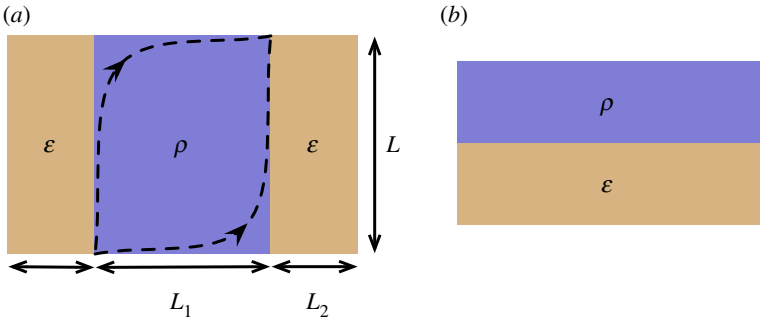

Figure 2. Different configurations of conductor–dielectric layered composites, where $\langle j_y \rangle = 0$ on the upper and lower boundaries, and we have periodic boundary conditions for the left and right boundaries. The interfaces between conductor ρ and dielectric ε can be perpendicular (*a*) or parallel (*b*) to the average current flow. The dashed lines in (*a*) are a schematic of the dominant current paths at large magnetic field $H \gg 1/\mu$ in the conductor. (Online version in colour.)

contacts in experiment. Indeed, a magnetocapacitance has already been observed in non-magnetic Schottky barriers [20].

In general, we find that the behaviour is strongly dependent on geometry. When the conductor–dielectric interfaces are parallel to the average current flow as in figure 2*b*, the dielectric response does not depend on magnetic field and we simply obtain $\varepsilon_{xx}(\omega) = \varepsilon + (\mathrm{i}\omega\rho)^{-1}$. By contrast, when the interfaces are perpendicular to the overall flow of charge as in figure 2*a*, the current becomes locally distorted, and we have a substantial magnetodielectric effect. First, at zero magnetic field, we recover the dielectric relaxation [21] expected from the Maxwell–Wagner effect—for a square unit with equal proportions of each phase, i.e. $L_1 = 2L_2 = L/2$ in figure 2*a*, this gives

$$\varepsilon_{xx}(\omega) = 2\varepsilon \frac{1 - \mathrm{i}\omega\tau}{1 + (\omega\tau)^2}, \tag{3.1}$$

where the time constant $\tau = \rho\varepsilon$. Here, at the characteristic frequency $\omega\tau = 1$, there is a rapid change in $\Re[\varepsilon_{xx}]$ and an associated peak in $\Im[\varepsilon_{xx}]$. Then, in the presence of a magnetic field, the peak shifts to smaller $\omega\tau$ with increasing β as shown in figure 3. Indeed, at large fields $\beta \gg 1$, the characteristic frequency becomes $\beta\omega\tau = 1$, and the behaviour evolves into a dielectric resonance, where the capacitance $\Re[\varepsilon_{xx}]$ can become negative. This is similar to the magnetocapacitance of isotropic composite media [8] considered in §4. We also obtain a similar magnetodielectric effect for other configurations of figure 2*a*, but the shift of the peak position in $\Im[\varepsilon_{xx}]$ often only approximately obeys $\beta\omega\tau = 1$.

To gain insights into this effect, we consider a modified version of the set-up in figure 2*a* where we insert a perfectly conducting metallic interface between the conductor and dielectric. Now, if we ignore the dielectric for the moment and consider DC transport through the conductor, then such boundary conditions will give rise to a magnetoresistance because of local current distortions at the boundaries [22]. In particular, if the conductor is square ($L_1 = L$), then the effective resistivity is exactly $\rho^*(H) = \rho\sqrt{1 + \beta^2}$ [4,23]. Thus, the response of the conductor–dielectric composite becomes (assuming $L_2 = L/2$)

$$\varepsilon_{xx}(\omega) = \frac{\varepsilon(1 - \mathrm{i}\omega\tau\sqrt{1 + \beta^2})}{1 + \omega^2\tau^2(1 + \beta^2)}. \tag{3.2}$$

In the limit $\beta \gg 1$, we essentially obtain Maxwell–Wagner relaxation with $\omega\tau$ replaced by $\beta\omega\tau$. Thus, we see that the effect of the interface is to mix the Hall component into the response (both real and imaginary parts) and replace ρ with the Hall resistivity $\rho\beta$. Note that we do not obtain a dielectric resonance here, and thus it appears that this feature requires non-zero Hall fields E_y within the dielectric itself, which is not the case for perfectly conducting interfaces.

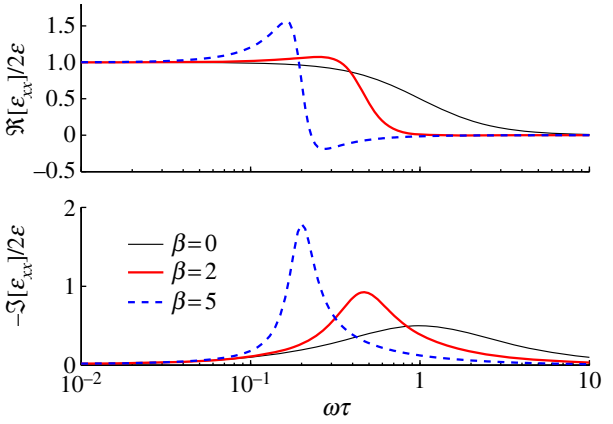

Figure 3. Magnetodielectric effect in conductor–dielectric layers for the geometry in figure 2*a* with $L_1 = 2L_2 = L/2$. For $\beta = 0$, we have ordinary Maxwell–Wagner dielectric relaxation, whereas for $\beta > 1$ it becomes a dielectric resonance with characteristic frequency $\beta\omega\tau = 1$. (Online version in colour.)

4. Isotropic composite media

We now turn to the dielectric response of a two-dimensional isotropic two-component medium where we once again have purely capacitive and purely resistive regions. When there are equal proportions of each component, we have the following exact results for the dielectric function [8]:

$$\varepsilon_{xx}(\omega) = \varepsilon \frac{(1 + \mathrm{i}\omega\tau)}{\sqrt{\mathrm{i}\omega\tau}\sqrt{(1 + \mathrm{i}\omega\tau)^2 - (\omega\tau\beta)^2}} \tag{4.1}$$

and

$$\varepsilon_{xy}(\omega) = \frac{\varepsilon}{\beta}\left(1 - \frac{\mathrm{i}}{\omega\tau}\right). \tag{4.2}$$

Referring to figure 4, we see that this also yields a dielectric resonance with characteristic frequency $\beta\omega\tau = 1$ for $\beta > 1$. However, note that $\varepsilon_{xx} \sim 1/\sqrt{\omega}$ in both low- and high-frequency limits, in contrast to the layered case with equal proportions. Moreover, the magnetodielectric effect for the isotropic medium appears to be smaller. This makes physical sense, because the isotropic medium contains interfaces in all different directions with respect to the average current flow, whereas our analysis of layered composites shows that the maximum effect is achieved when the interface is perpendicular to the flow. This suggests that we can enhance the magnetodielectric effect by having a system with multiple conductor–dielectric interfaces that are all perpendicular to the overall current flow.

We can also allow for the possibility that the resistive component has an intrinsic magnetoresistance $\rho_{xx}(H)$ by considering the more general expression for the resistivity tensor in equation (2.1). In this case, we obtain

$$\varepsilon_{xx}(\omega) = \varepsilon \frac{1 + \mathrm{i}\omega\varepsilon\rho_{xx}}{\sqrt{\mathrm{i}\omega\varepsilon\rho_{xx}}\sqrt{(1 + \mathrm{i}\omega\varepsilon\rho_{xx})^2 - \omega^2\varepsilon^2\rho_{xy}^2}}. \tag{4.3}$$

Here, we find that the size of the magnetocapacitance (i.e. the change of $\Re[\varepsilon_{xx}(\omega)]/\varepsilon$ with β) depends crucially on the ratio ρ_{xy}/ρ_{xx}. Thus, we can have an enhanced magnetocapacitance for a *negative* intrinsic magnetoresistance, where $\rho_{xy}/\rho_{xx} \sim \rho\beta/\rho_{xx}$ is large at finite magnetic field. However, without a Hall component (i.e. $\rho_{xy} = 0$), we simply have $\varepsilon_{xx}(\omega) = \varepsilon/\sqrt{\mathrm{i}\omega\epsilon\rho_{xx}}$, and we have only a magnetocapacitance when there is an intrinsic magnetoresistance $\rho_{xx}(H)$. In this case, we have no relaxation or resonance phenomena.

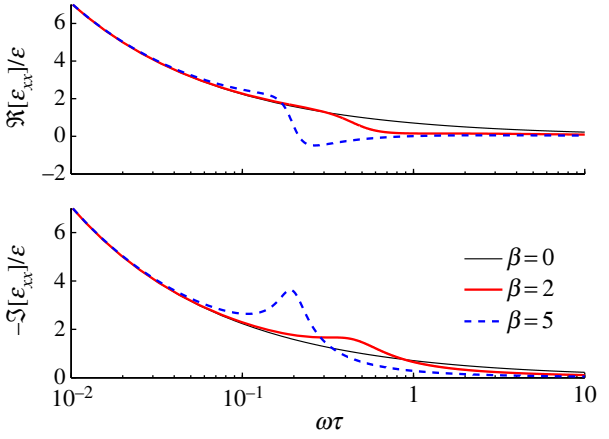

Figure 4. Magnetodielectric effect in isotropic conductor–dielectric composites with equal volume fractions. For $\beta > 1$, there is a dielectric resonance with characteristic frequency $\beta\omega\tau = 1$ that is superimposed on the $1/\sqrt{\omega\tau}$ behaviour expected at $\beta = 0$. (Online version in colour.)

(a) Effective medium approximation

To investigate all volume fractions of the components, we use the self-consistent effective medium approximation. Following Magier & Bergman [16], we simplify the problem by first transforming to a frame where the resistivity tensors of each phase are scalar. Thus, we take

$$\mathbf{E}' = \mathbf{E} + b\hat{R}\rho\mathbf{J} \tag{4.4}$$

and

$$\mathbf{J}' = c\mathbf{J} + \hat{R}\rho^{-1}\mathbf{E}, \tag{4.5}$$

where $\hat{R}$ is a rotation by 90 degrees,

$$\hat{R} = \begin{pmatrix} 0 & -1 \\ 1 & 0 \end{pmatrix}, \tag{4.6}$$

and the transformation constants are

$$b = \frac{1}{2\rho_{xy}\rho}\left[\rho_{xx}^2 + \rho_{xy}^2 + \frac{\rho^2}{(\omega\tau)^2} + \sqrt{\left(\rho_{xx}^2 + \rho_{xy}^2 + \frac{\rho^2}{(\omega\tau)^2}\right)^2 - 4\frac{\rho_{xy}^2\rho^2}{(\omega\tau)^2}}\right]$$

$$c = -\frac{1}{2\rho_{xy}\rho}\left[\rho_{xx}^2 + \rho_{xy}^2 + \frac{\rho^2}{(\omega\tau)^2} - \sqrt{\left(\rho_{xx}^2 + \rho_{xy}^2 + \frac{\rho^2}{(\omega\tau)^2}\right)^2 - 4\frac{\rho_{xy}^2\rho^2}{(\omega\tau)^2}}\right],$$

using equation (2.1) for the first component $\hat{\rho}_1$. Note that these coefficients are real, even though the dielectric phase (component 2) has a purely imaginary resistivity, $\rho_2 = (\mathrm{i}\omega\varepsilon)^{-1}$. In the transformed frame, the (dimensionless) resistivities of the two components are

$$\frac{\rho_1'}{\rho} = \frac{\rho_{xx}}{\rho_{xy} + \rho c}, \quad \frac{\rho_2'}{\rho} = -\frac{\mathrm{i}}{\omega\tau c}.$$

From equation (2.2), the effective resistivity of the transformed composite is then

$$\rho_e' = \left(\frac{1}{2} - p\right)(\rho_1' - \rho_2') + \sqrt{\left(\frac{1}{2} - p\right)^2(\rho_1' - \rho_2')^2 + \rho_1'\rho_2'}, \tag{4.7}$$

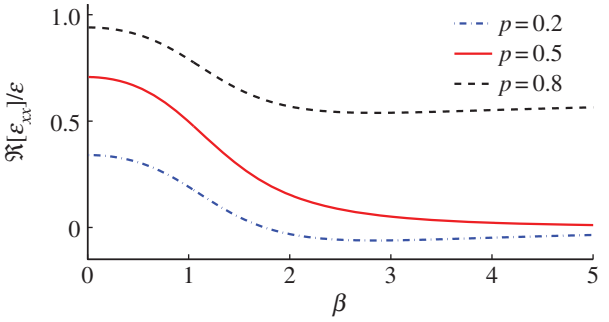

Figure 5. Magnetocapacitance of isotropic conductor–dielectric composites at fixed frequency $\omega\tau = 1$ for different dielectric volume fractions p. In the limit of high magnetic field $\beta \to \infty$, $\Re[\varepsilon_{xx}]/\varepsilon \to 0$ and $\Re[\varepsilon_{xx}]/\varepsilon \to 2p - 1$ for $p \leq 1/2$ and $p > 1/2$, respectively. (Online version in colour.)

where p is the volume fraction of the dielectric phase. Transforming back to the original frame then yields the final result for the longitudinal effective resistivity,

$$\frac{\rho_{e,xx}}{\rho} = \frac{\rho\rho_e'}{\rho^2 + (\rho_e')^2}(b + c). \tag{4.8}$$

Note that taking equal proportions ($p = 1/2$) yields the exact result described earlier—we can recover equation (4.3) using $\epsilon_{xx}(\omega) = (\mathrm{i}\omega\rho_{e,xx})^{-1}$. In what follows, we assume that we simply have $\rho_{xx} = \rho$ and $\rho_{xy} = \beta\rho$.

For all volume fractions p, one can show that there is always a dielectric resonance at $\beta\omega\tau = 1$ for large magnetic fields [8]. Moreover, we find that the dissipation at the peak only depends on p to leading order in β,

$$\frac{\rho_{e,xx}}{\rho} \simeq \frac{2}{1 - 2p + \sqrt{1 + 4p(1-p)}} + \mathrm{i}O\left(\frac{1}{\beta}\right), \tag{4.9}$$

where we see that $\rho_{e,xx}/\rho \to \infty$ when $p \to 1$, as expected. Contrast this with the layered case (e.g. equation (3.2)), where we find that $\rho_{e,xx}/\rho$ at the peak increases with increasing magnetic field β.

If we fix the frequency ω, then we also find a sizeable magnetocapacitance that depends on p. Figure 5 depicts the magnetocapacitance for $\omega\tau = 1$, and we see that both the size and sign of $\Re[\varepsilon_{xx}]/\varepsilon$ at large β is determined by p. Indeed, in the limit $\beta \to \infty$, $\Re[\varepsilon_{xx}]/\varepsilon$ only remains finite when $p > 1/2$, and the dielectric phase percolates through the whole sample.

Further insights can be obtained by deriving the limiting behaviour of the AC response from equation (4.8). Let us first consider the case where the magnetic field $\beta = 0$. Then, in the limit $\omega\tau \to 0$, we have

$$\frac{\rho_{e,xx}}{\rho} \simeq \begin{cases} \dfrac{1}{1-2p}, & p < \dfrac{1}{2} \\ \dfrac{\mathrm{i}}{\omega\tau}(1-2p), & p > \dfrac{1}{2}. \end{cases} \tag{4.10}$$

Likewise, in the limit $\omega\tau \to \infty$, we have

$$\frac{\rho_{e,xx}}{\rho} \simeq \begin{cases} 1-2p, & p < \dfrac{1}{2} \\ \dfrac{\mathrm{i}}{\omega\tau}\dfrac{1}{1-2p}, & p > \dfrac{1}{2}. \end{cases} \tag{4.11}$$

Here, we can clearly see the effect of percolation, because the conducting regions dominate the transport below the percolation threshold of the dielectric ($p < 1/2$), whereas the dielectric regions dominate above ($p > 1/2$). In particular, we see that the dependence on p is inverted for low and high frequencies, because the dielectric regions effectively behave insulating in the former

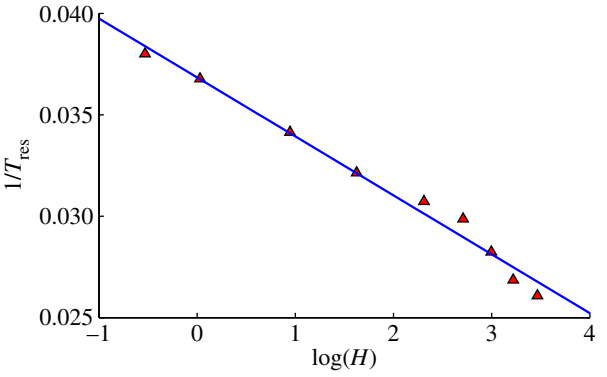

Figure 6. Position of the resonance peak in the imaginary part of the dielectric response in terms of inverse temperature $1/T$ as a function of magnetic field H. Triangles are data for nanoporous silicon taken from Brooks *et al.* [11], whereas the line corresponds to a fit from our classical model of conductor–dielectric composites. (Online version in colour.)

case and metallic in the latter (where there is insufficient time for the dielectric to build up charge). However, for the special case $p = 1/2$, i.e. at the percolation threshold, we simply have $\rho_{e,xx} = \rho/\sqrt{\mathrm{i}\omega\tau}$ and thus the same behaviour in both limits.

When there is a large magnetic field ($\beta \gg 1$), we obtain the same result for $\omega\tau \to 0$, or $\beta\omega\tau \ll 1$, but there can be markedly different behaviour when $\beta\omega\tau \gtrsim 1$. Specifically, for $\beta \to \infty$ and finite $\omega\tau$, we obtain

$$\frac{\rho_{e,xx}}{\rho} \simeq \begin{cases} \dfrac{1}{1-2p}, & p < \dfrac{1}{2} \\ \dfrac{\beta\sqrt{\mathrm{i}\omega\tau}}{1+\mathrm{i}\omega\tau}, & p = \dfrac{1}{2} \\ \dfrac{\mathrm{i}}{\omega\tau}\dfrac{1}{1-2p}, & p > \dfrac{1}{2}, \end{cases} \tag{4.12}$$

which matches the large β behaviour in figure 5. Note that, for $p < 1/2$, the system at high frequencies behaves like one at low frequencies (equation (4.10)). This implies that the dielectric region behaves insulating rather than metallic as one might normally expect at high frequencies. This is because, at large magnetic field, the current paths are distorted such that they avoid any metallic region (cf. [5]) and thus any metal effectively behaves like an insulator.

5. Discussion

The dielectric response investigated in this paper depends only on the presence of macroscopic inhomogeneities and can thus potentially be observed in a variety of materials. There is already evidence to suggest that it accounts for the magnetodielectric effect in graphene–polyvinyl alcohol nanocomposite films [24] and in nickel nanosheet–Na-4 mica composites [25]. Furthermore, our results are possibly relevant to rough interfaces in heterostructures [26].

Experiments on nanoporous silicon [10,11] have revealed a magnetic-field-dependent dielectric resonance that is consistent with our model. In this case, the dielectric response was measured at fixed frequency $\omega = 100\,\mathrm{kHz}$ as a function of temperature $T = 25$–$40\,\mathrm{K}$ and magnetic field $H = 0$–$32\,T$. However, varying the temperature is equivalent to varying $\omega\tau$ if we approximate ε as temperature independent and the electrical transport in the semiconductor as being activated: $\rho = \rho_0 e^{\Delta/k_B T}$, where Δ is the activation gap. Then, our predicted resonance occurs at the temperature $k_B T = -\Delta/\log(\beta\omega\varepsilon\rho_0)$, so that the dielectric resonance shifts to higher T with increasing H, as indeed was observed in experiment. Assuming that $\beta = 1$ corresponds to $H \simeq 1\,T$, we can fit the data with $\omega_0 \equiv 1/\rho_0\varepsilon \simeq 4 \times 10^{10}\,\mathrm{Hz}$ and $\Delta \simeq 30\,\mathrm{meV}$, as shown in figure 6. Note that the size of Δ is consistent with activation from an impurity band.

Our effect may also be relevant to the dielectric resonance observed in the manganite $La_{2/3}Ca_{1/3}MnO_3$ just above the ferromagnetic transition temperature [12]. However, here the situation is more complex, because there is magnetism involved and the effective 'composite' corresponds to the phase separation between magnetic metal and charge-ordered insulator. Moreover, the size of magnetic metallic domains could change with magnetic field. This all requires further investigation: in principle, one might be able to probe the latter possibility by measuring the Hall component ε_{xy}, as discussed in Parish & Littlewood [8].

Finally, with regards to experiment, there is the issue of when our classical model breaks down as the size of the sample is reduced. Formally, our approach is only valid when $1/\omega$ is greater than any microscopic time scale, e.g. the scattering time of charge carriers within the conducting regions, and when the size of the inhomogeneities is greater than any microscopic length scale, e.g. mean free path. However, one may be able to extend our results to smaller sizes using an appropriately redefined ε and $\hat{\rho}$.

6. Conclusion

In this paper, we have investigated two-dimensional conductor–dielectric composites and we have shown how these can produce a magnetic-field-dependent dielectric response without any magnetism. Using exact results and the effective medium approximation, we have derived expressions for the dielectric response of isotropic composite media and we have explicitly revealed the behaviour at the resonance $\beta\omega\tau = 1$ and in the limits $\omega\tau \to 0$, $\omega\tau \to \infty$ and $\beta \to \infty$. Moreover, we find that an intrinsic magnetoresistance could enhance this magnetodielectric effect from inhomogeneities. We have also performed numerical simulations of layered composites to show that conductor–dielectric interfaces play a key role in this phenomenon. Based on these results, we expect the magnetodielectric effect to be largest in a system with conductor–dielectric interfaces that are all perpendicular to the overall current flow. Finally, we have discussed how our predicted magnetodielectric effect has already been observed experimentally in some materials. A remaining question is why our two-dimensional calculation appears to be so successful at describing three-dimensional systems in experiment. Certainly, if the dominant effect is from conductor–dielectric interfaces, then this should be captured by a two-dimensional model. However, it is known that a non-saturating magnetoresistance can be generated by the effects of three-dimensional geometry alone [23]. One possible resolution is that three-dimensional geometrical effects can be mapped onto an effective two-dimensional model—it has already been shown that a sample consisting of different thicknesses can be described by a two-dimensional system of components with different resistivities [27]. An investigation of how our results generalize to higher dimensions will be the subject of future work.

Acknowledgements. I am grateful to Peter Littlewood for fruitful discussions.

Funding statement. This work was supported by the EPSRC under grant no. EP/H00369X/2.

References

1. Xu R, Husmann A, Rosenbaum TF, Saboungi M-L, Enderby JE, Littlewood PB. 1997 Large magnetoresistance in non-magnetic silver chalcogenides. *Nature* **390**, 57–60. (doi:10.1038/36306)
2. Husmann A, Betts JB, Boebinger GS, Migliori A, Rosenbaum TF, Saboungi M-L. 2002 Megagauss sensors. *Nature* **417**, 421–424. (doi:10.1038/417421a)
3. Parish MM, Littlewood PB. 2003 Non-saturating magnetoresistance in heavily disordered semiconductors. *Nature* **426**, 162–165. (doi:10.1038/nature02073)
4. Parish MM, Littlewood PB. 2005 Classical magnetotransport of inhomogeneous conductors. *Phys. Rev. B* **72**, 094417. (doi:10.1103/PhysRevB.72.094417)
5. Solin SA, Thio T, Hines DR, Heremans JJ. 2000 Enhanced room-temperature geometric magnetoresistance in inhomogeneous narrow-gap semiconductors. *Science* **289**, 1530–1532. (doi:10.1126/science.289.5484.1530)

6. Zhou T, Solin SA, Hines DR. 2001 Extraordinary magnetoresistance in externally shunted van der Pauw plates. *Appl. Phys. Lett.* **78**, 667. (doi:10.1063/1.1343472)
7. Catalan G. 2006 Magnetocapacitance without magnetoelectic coupling. *Appl. Phys. Lett.* **88**, 102902. (doi:10.1063/1.2177543)
8. Parish MM, Littlewood PB. 2008 Magnetocapacitance in nonmagnetic composite media. *Phys. Rev. Lett.* **101**, 166602. (doi:10.1103/PhysRevLett.101.166602)
9. Eerenstein W, Mathur ND, Scott JF. 2006 Multiferroic and magnetoelectric materials. *Nature* **442**, 759–765. (doi:10.1038/nature05023)
10. Vasic R, Brooks JS, Jobiliong E, Aravamudhan S, Luongo K, Bhansali S. 2007 Dielectric relaxation in nanopillar NiFe–silicon structures in high magnetic fields. *Curr. Appl. Phys.* **7**, 34–38. (doi:10.1016/j.cap.2005.08.002)
11. Brooks JS, Vasic R, Kismarahardja A, Steven E, Tokumoto T, Schlottmann P, Kelly S. 2008 Debye relaxation in high magnetic fields. *Phys. Rev. B* **78**, 045205-1–045206. (doi:10.1103/PhysRevB.78.045205)
12. Rivas J, Mira J, Rivas-Murias B, Fondado A, Dec J, Kleemann W, Senaris Rodriguez MA. 2006 Magnetic field-dependent dielectric constant in $La_{2/3}Ca_{1/3}MnO_3$. *Appl. Phys. Lett.* **88**, 242906. (doi:10.1063/1.2213513)
13. Maglione M. 2008 Interface-driven magnetocapacitance in a broad range of materials. *J. Phys. Condens. Matter* **20**, 322202. (doi:10.1088/0953-8984/20/32/322202)
14. Stroud D. 1975 Generalized effective-medium approach to the conductivity of an inhomogeneous material. *Phys. Rev. B* **12**, 3368–3373. (doi:10.1103/PhysRevB.12.3368)
15. Guttal V, Stroud D. 2005 Model for a macroscopically disordered conductor with an exactly linear high-field magnetoresistance. *Phys. Rev. B* **71**, 201304. (doi:10.1103/PhysRevB.71.201304)
16. Magier R, Bergman DJ. 2006 Strong-field magnetotransport of two-phase disordered media in two and three dimensions: exact and approximate results. *Phys. Rev. B* **74**, 094423. (doi:10.1103/PhysRevB.74.094423)
17. Dykhne AM. 1971 Anomalous plasma resistance in a strong magnetic field. *Sov. Phys. JETP* **32**, 348.
18. Balagurov BYa. 1978 Galvanomagnetic properties of thin inhomogeneous films. *Sov. Phys. Solid State* **20**, 1922.
19. Dykhne AM, Ruzin IM. 1994 Theory of the fractional quantum Hall effect: the two-phase model. *Phys. Rev. B* **50**, 2369. (doi:10.1103/PhysRevB.50.2369)
20. Tongay S, Hebard AF, Hikita Y, Hwang HY. 2009 Magnetodielectric coupling in nonmagnetic Au/GaAs:Si Schottky barriers. *Phys. Rev. B* **80**, 205324. (doi:10.1103/PhysRevB.80.205324)
21. Jonscher AK. 1983 *Dielectric relaxation in solids*. London, UK: Chelsea Dielectrics Press.
22. Pippard AB. 1989 *Magnetoresistance in metals*. Cambridge, UK: Cambridge University Press.
23. Isichenko MB, Kalda J. 1992 Shape effects of magnetoresistance. *J. Moscow Phys. Soc.* **2**, 55–69.
24. Mitra S, Mondal O, Saha DR, Datta A, Banerjee S, Chakravorty D. 2011 Magnetodielectric effect in graphene–PVA nanocomposites. *J. Phys. Chem. C* **115**, 14 285–14 289. (doi:10.1021/jp203724f)
25. Mitra S, Mandal A, Datta A, Banerjee S, Chakravorty D. 2010 Magnetodielectric effect in nickel nanosheet-Na-4 mica composites. *Europhys. Lett.* **92**, 26003. (doi:10.1209/0295-5075/92/26003)
26. Dussan S, Kumar A, Scott JF, Katiyar RS. 2010 Magnetic effects on dielectric and polarization behavior of multiferroic heterostructures. *Appl. Phys. Lett.* **96**, 072904. (doi:10.1063/1.3327889)
27. Bruls GJCL, Bass J, van Gelder AP, van Kempen H, Wyder P. 1981 Linear magnetoresistance caused by sample thickness variations. *Phys. Rev. Lett.* **46**, 553–555. (doi:10.1103/PhysRevLett.46.553)